Abrupt Transition between Three-Dimensional and Two-Dimensional Quantum Turbulence

Nicolás P. Müller,[1,3] Marc-Etienne Brachet,[2] Alexandros Alexakis,[2] and Pablo D. Mininni[1]
[1]Universidad de Buenos Aires, Facultad de Ciencias Exactas y Naturales, Departamento de Física, & IFIBA, CONICET, Ciudad Universitaria, Buenos Aires 1428, Argentina
[2]Laboratoire de Physique de l'École Normale Supérieure, ENS, Université PSL, CNRS, Sorbonne Université, Université de Paris, F-75005 Paris, France
[3]Université Côte d'Azur, Observatoire de la Côte d'Azur, CNRS, Laboratoire Lagrange, Bd de l'Observatoire, CS 34229, 06304 Nice Cedex 4, France

(Received 8 November 2019; revised manuscript received 6 February 2020; accepted 7 March 2020; published 31 March 2020)

We present numerical evidence of a critical-like transition in an out-of-equilibrium mean-field description of a quantum system. By numerically solving the Gross-Pitaevskii equation we show that quantum turbulence displays an abrupt change between three-dimensional (3D) and two-dimensional (2D) behavior. The transition is observed both in quasi-2D flows in cubic domains (controlled by the amplitude of a 3D perturbation to the flow), as well as in flows in thin domains (controlled by the domain aspect ratio) in a configuration that mimics systems realized in laboratory experiments. In one regime the system displays a transfer of the energy towards smaller scales, while in the other the system displays a transfer of the energy towards larger scales and a coherent self-organization of the quantized vortices.

DOI: 10.1103/PhysRevLett.124.134501

The phenomena of condensation and phase transitions in statistical mechanics has traditionally been associated with equilibria. However, observations of turbulence in experiments of gaseous Bose-Einstein condensates (BECs) [1–3] and of superfluid ^{4}He [4–6] have shown that these out-of-equilibrium systems can also display multiple phases. In particular, recent BEC experiments close to a two-dimensional (2D) regime, instead of a tendency towards disorder, display an intriguing out-of-equilibrium self-organization and the nucleation of quantized vortices [7–9] (see Refs. [10,11] for numerical studies).

In classical turbulence, a reminiscent process can take place when flows are 2D. Under certain conditions, the kinetic energy can undergo an inverse cascade (moving to larger scales), and eventually create a condensate [12]. This condensation is of a different nature than a BEC as it involves the kinetic energy of the system instead of its mass density. In classical three-dimensional (3D) turbulence, recent developments indicate that this far-from-equilibrium system can change its behavior as its dimensionality is changed [13–16] (or, equivalently, as one of its spatial dimensions is compactified, see Ref. [13], and Ref. [17] for an example of a transition under compactification in gravitational theories). In classical fluids, when the flow is 3D energy undergoes a direct cascade (moving to smaller scales), while as the domain that contains the fluid is made thiner, the system becomes 2D and displays an inverse cascade after a critical second-order transition.

Both classical and quantum turbulence involve nonlinear and complex spatiotemporal dynamics of fields, and cascadelike solutions can develop in many different cases. In this Letter we address the following questions: Is there a transition in the behavior of quantum turbulence as its dimensionality is changed as reported in recent quantum turbulence experiments [7–9]? And is this transition associated with the emergence of different out-of-equilibrium self-similar regimes (i.e., associated with a change in the direction of the energy cascade)? To this end, we study numerically 3D condensates in periodic boundary conditions using the Gross-Pitaevskii equation (GPE), exploring two configurations. In one, we solve the equations in a cubic domain and perturb an initial 2D random array of quantized vortices with a 3D perturbation, varying the amplitude of the perturbation as a control parameter. In the other, we consider a quasi-2D array of quantized vortices and vary the aspect ratio of the domain, compactifying one of its dimensions. In both cases we find evidence of an abrupt transition towards a regime that displays two-dimensionalization, spatial aggregation of quantized vortices, and inverse energy flux.

To describe the dynamics of weakly interacting bosons of mass m at zero temperature we solve numerically the GPE [18], $i\hbar\partial_t\psi = -\hbar^2\nabla^2\psi/(2m) + g|\psi|^2\psi$, where ψ is the condensate wave function and g is proportional to the scattering length. The fluid density, velocity, and quantized vortices can be obtained from ψ using Madelung's transformation (see Ref. [18]). The GPE is solved using a parallel pseudospectral method [19,20]. To achieve the largest possible scale separation (at a fixed spatial resolution), we resort to periodic boundary

conditions in a 3D domain of size $L_x \times L_y \times L_z$, with spatial resolution $N_x \times N_y \times N_z$. The size of the domain is $L_x = L_y = L_\perp = 2\pi$ in dimensionless units in all cases, and $L_z = \gamma L_\perp$, where γ is the domain aspect ratio. In these domains, we prepared a set of randomly distributed 2D vortices with a small 3D perturbation of amplitude A_z, such that the wave function is a solution of the GPE, and that the incompressible kinetic energy of the system peaks at an intermediate wave number $k_0 \approx 10$ (i.e., the correlation length of the flow is $\ell_0 \approx L_\perp/10$; see Ref. [18] for more details on the preparation of the initial conditions and for the definition of the incompressible kinetic energy). This results in quantized vortices with a random separation, and that are perfectly 2D for $A_z = 0$ while they display stronger curvature in z for increasing A_z.

As previously mentioned, we consider two ways to observe a transition between 2D and 3D flows using these initial conditions. One of them consists in varying the amplitude of the 3D perturbation A_z between 0 and 1 in a cubic domain. The other is to vary the aspect ratio of the domain for fixed A_z (the 2D limit case being that in which $\gamma = L_z/L_\perp \to 0$, and the 3D case when $\gamma = 1$). In each case, when varying the control parameters between their two limits, classically we can expect an inverse cascade of energy in the 2D regime, and the absence thereof in the 3D case. To identify the direction of the cascades we consider two quantities: the incompressible kinetic energy spectrum $E_k^i(k)$ (see Refs. [18,21,22] for a detailed description of energy components in the GPE) and the total energy flux $\Pi(k) = -dE^<(k)/dt$, where $E^<(k)$ is the total energy of the system integrated up to wave number k, $E^<(k) = \int_0^k E(k')dk'$, and where $E(k)$ is the total energy spectrum [18]. A direct cascade of energy corresponds to the development of a power law in $E_k^i(k)$ for $k > k_0$ and with $\Pi(k) > 0$ constant in a range of wave numbers, while an inverse cascade of energy corresponds to a growth of $E_k^i(k)$ for $k < k_0$ and with $\Pi(k) < 0$. As the system has no external steering force (but no dissipation either), an inverse cascade can only develop for a transient time [23], and in the following we will focus on time averages of these quantities between $t = 1$ and 10 flow turnover times, as well as on their time evolution over the same time span (with the turnover time defined as $\tau = \ell_0/U$, with U the rms initial flow velocity).

In cubic domains ($\gamma = 1$) we performed two sets of simulations, with spatial resolutions of $N_x \times N_y \times N_z = 256^3$ and 512^3 grid points, varying the amplitude of the 3D perturbation A_z. For large values of A_z the flow quickly evolves into a 3D regime, with quantized vortices rapidly being deformed, while for small A_z there is a long transient in which the flow remains quasi-2D (see the videos in Ref. [18]). Figure 1(a) shows the time average of $E_k^i(k)$ for the simulations with 512^3 grid points, and for different values of A_z. For large values of A_z initial vertical gradients in the quantized vortices are large, and the spectrum peaks at $k \approx k_0$ followed by a spectrum compatible with a direct energy cascade and with the emission of Kelvin waves at wave numbers smaller than the inverse mean intervortex distance [20]. The energy fluxes in Fig. 1(b), specially for $A_z = 1$, are positive for all k and remain approximately constant for a range of wave numbers $k > k_0$. But for small values of A_z initial vertical gradients are small, and the energy spectrum grows for $k \lesssim k_0$, developing a power law compatible with Kolmogorov scaling, and with negative total energy flux for $k \lesssim k_0$ (albeit the negative flux does not remain constant with k, as a result of limited spatial resolution and of the inverse cascade being only transient in the absence of external forcing). In spite of this, the system

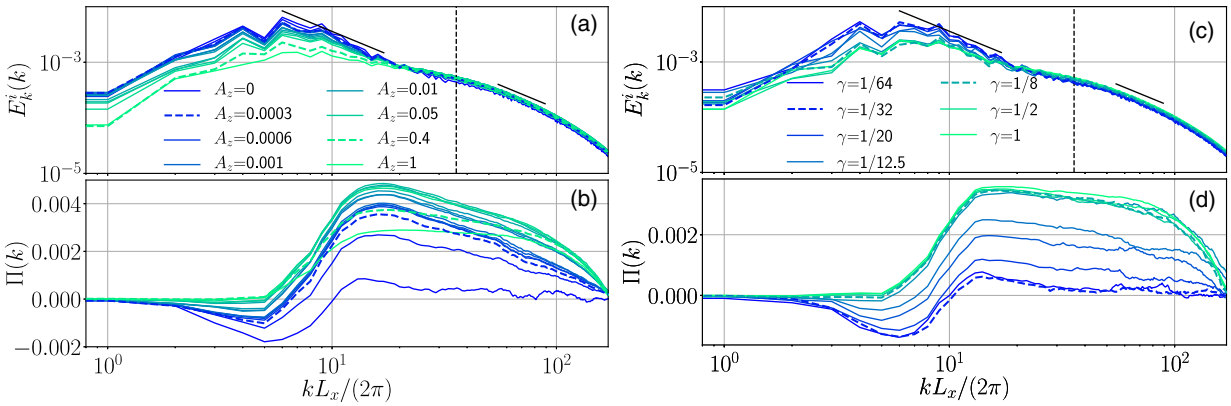

FIG. 1. (a) Spectrum of the incompressible kinetic energy averaged between $t = 1$ and 10 for simulations in cubic domains ($N_x = N_y = N_z = 512$) and different values of A_z. Kolmogorov power laws $\sim k^{-5/3}$ are indicated as a reference by solid black lines. The vertical dashed line indicates the inverse mean intervortex distance. Note the growth of energy and a $\sim k^{-5/3}$ scaling for $k \lesssim 10$ when A_z is small. (b) Total energy fluxes for the same simulations. For small A_z the flux becomes negative for $k \lesssim 10$, and the positive flux for $k > 10$ decreases. References for the values of A_z in (a) and (b) are provided in the inset. (c) Same as in (a) for simulations in thin domains, for different values of γ. (d) Same as in (c) for simulations in thin domains; the inset gives the values of γ. In all panels, dashed curves highlight simulations for which movies are available in Ref. [18].

develops a strong inverse transfer of energy, at least up to $t = 10$. For longer times the flow eventually becomes unstable and 3D. However, we verified that the 2D behavior is not simply due to an absence of 3D motions for $A_z \ll 1$. For $t \lesssim 10$, when the systems display an inverse transfer of energy, the energy in the 3D modes for all $A_z \neq 0$ is significant enough to nonlinearly act back to the 2D part of the flow and saturate its initial exponential growth, but not strong enough yet to suppress the inverse transfer.

Figures 1(c) and 1(d) show similar results for simulations with a fixed value of $A_z = 0.1$ (such that a 3D flow with a direct energy cascade is generated when $\gamma = 1$), but with different aspect ratios γ, using a spatial resolution $N_x = N_y = 512$, and with N_z varied between 512 and 32 grid points to keep the vertical resolution Δz fixed or over-resolved as L_z is decreased, so that vertical gradients in the flow are always correctly resolved. Although the amplitude of the perturbation A_z is fixed, by decreasing γ we also increase the wave number of the vertical perturbation (i.e., vertical variations of quantized vortices increase as the domain becomes thinner). As in the cubic domain, we observe an increase in $E_k^i(k)$ for $k \lesssim k_0$ and a range of wave numbers with $\Pi(k) < 0$ but now for small values of γ, and a direct cascade of energy for large values of γ. But, unlike the case of the cubic domain, when γ is sufficiently small the flow remains quasi-2D for very long times, and quantized vortices aggregate in physical space creating larger structures (see movies in the Supplemental Material [18]).

To quantify the transition between the direct and inverse cascade regimes, we need to use (as an order parameter) an observable that measures the relative strength of the inverse energy cascade. To this end we first introduce the mean inverse flux at small wave numbers (which is zero when the flux is positive), and the mean direct flux at large wave numbers, respectively, defined as

$$\Pi^{<} = \left| \min \left\{ 0, \frac{1}{k_0} \sum_{k=0}^{k_0} \Pi(k) \right\} \right|, \tag{1}$$

$$\Pi^{>} = \frac{1}{k_{\max} - (k_0 + 1)} \sum_{k=k_0+1}^{k_{\max}} \Pi(k), \tag{2}$$

where $k_{\max} = N_x/3$ is the maximum resolved wave number in the simulations, and k_0 is as before the wave number where the incompressible kinetic energy is initially concentrated. We can then compute the total energy flux (in both directions) $\Pi^{\text{tot}} = \Pi^{<} + \Pi^{>}$, and define the normalized ratio of inverse energy flux to total energy flux $\Pi^{<}/\Pi^{\text{tot}}$. Figure 2 shows the behavior of this quantity for all cases studied, as a function of the amplitude of the 3D perturbation normalized by its critical value A_z/A_z^c (for spatial resolutions of 256^3 and 512^3 grid points), and as a function of the aspect ratio normalized by its critical value

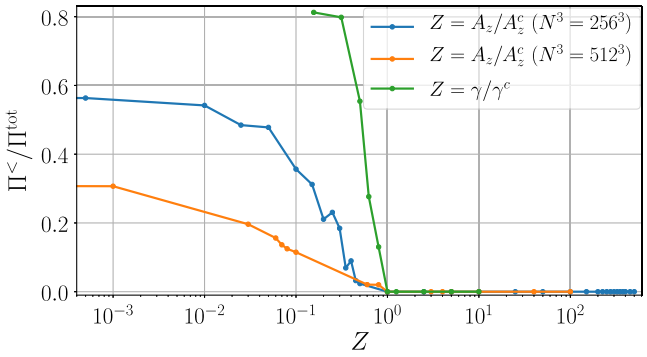

FIG. 2. Ratio of inverse energy flux to total energy flux as a function of the normalized control parameter Z (either A_z or γ, normalized by their respective critical values A_z^c or γ^c, see inset). For cubic domains two curves are shown, corresponding to spatial resolutions of 256^3 and 512^3 grid points.

γ/γ^c (for fixed A_z). In all cases we see an abrupt change as the control parameter is varied. For A_z/A_z^c or $\gamma/\gamma^c > 1$ there is no inverse energy flux, while for A_z/A_z^c or $\gamma/\gamma^c < 1$ it grows rapidly (albeit differently in each case). In the thin domains, from Fig. 1 it can be seen that $\gamma^c \approx 0.1$, corresponding to a domain with $L_z = L_\perp/10 \approx 11\xi$ (where ξ is the healing length of the condensate, proportional to the vortex core radius). This implies that the 2D behavior occurs when the height of the domain is of the same order as the correlation of the initial conditions, $\gamma_c \simeq \ell_0/L_\perp$, a similar condition for the layer height and the forcing length scale found for the compactified case in classical flows [13]. In other words, a transition towards 2D behavior does not require 2D domains or very slim films. Even moderate aspect ratios are enough to trigger an inverse energy cascade.

Energy fluxes, although they give a direct indication of the presence of an inverse cascade, are not easily measurable in laboratory experiments. There are, however, other global quantities that are tractable experimentally and can also give an indication of a transition from 3D to 2D behavior in the flows as the control parameters are varied. Figure 3 shows the incompressible kinetic energy E_{inc} in these flows as a function of time, both for 512^3 simulations in cubic boxes with different A_z as well as for simulations in domains with different γ, and for each case, also the total length of the vortices as a function of time. In the simulations with large A_z or γ, E_{inc} decays in time after $t \approx 1$, as the direct cascade of energy transfers the incompressible kinetic energy to smaller scales where it dissipates into phonons [20,21,24]. However, for small A_z or γ, E_{inc} remains constant in time or decays very slowly, indicating energy remains at large scales as in classical 2D turbulence. The same behavior is seen in the total vortex length [18,21], which grows and reaches a maximum in the 3D regime as a result of vortex stretching (later decaying as a result of vortex reconnection), but which remains approximately constant for all times in the cases of small A_z or γ, pointing

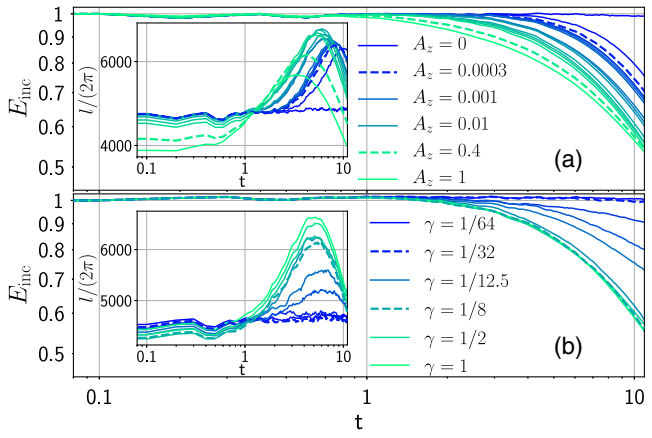

FIG. 3. Time evolution of the incompressible kinetic energy (a) in simulations in cubic domains with different perturbation amplitudes A_z (512^3 runs), and (b) in simulations in domains with different aspect ratios γ. The insets show the total vortex length [18] as a function of time for each case. References are as in Fig. 1; a few labels are provided as guidelines.

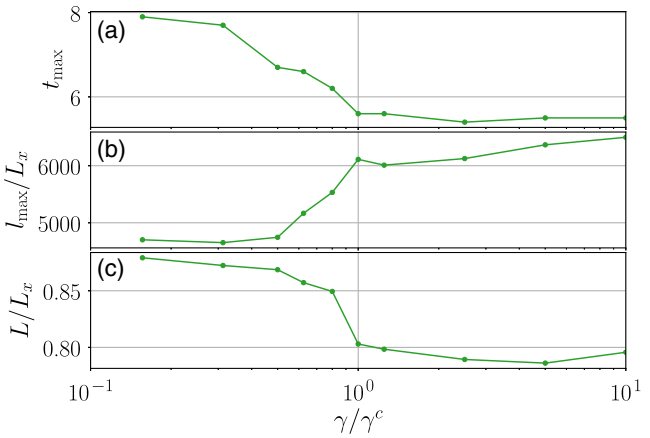

FIG. 4. (a) Time to reach the maximum length of the vortices as a function of γ/γ^c. (b) Normalized maximum total length of the vortices, $l_{\rm max}/L_x$, as a function of the control parameter. (c) Flow integral length scale normalized by the domain size, L/L_x, as a function of the same control parameter.

to the absence of vortex stretching as expected in 2D flows. Vortex reconnection also plays an important role at early times for large A_z or γ, to speed-up the three-dimensionalization of the flow, after which vortex stretching can become more efficient. Finally, it is also important to note that in the simulations in cubic domains the total length of the vortices remains approximately constant at early times in all cases, and that the time when vortex stretching starts increases as A_z decreases. This is consistent with our previous observations: In the cubic box, for smaller values of A_z the flow remains quasi-2D for longer times, and the observed transient inverse cascade delays the growth of 3D excitations in the flow.

Given the above we can consider various quantities that can indicate the presence of a sharp transition. Here we focus only on the thin layer case that is somehow closer to what is experimentally realizable. Figure 4 shows the time to reach the maximum vortex stretching $t_{\rm max}$, the maximum length of the vortices $l_{\rm max}$, and the flow integral scale L as a function of γ, which is obtained from the incompressible kinetic energy spectrum as $L = 2\pi \int k^{-1} E_k^i(k) dk / \int E_k^i(k) dk$, and provides an estimation of the flow energy containing scale. When $L \approx L_x$ (the domain size), the flow has self-organized at the largest available scale in the domain. These quantities display an abrupt change near the critical value γ^c as γ is varied. The time $t_{\rm max}$ is larger when $\gamma < \gamma^c$, while the maximum vortex length is larger when $\gamma > \gamma^c$. Both behaviors are to be expected when the flow is 3D and displays vortex stretching, or when the flow is 2D and as a result does not. Finally, the flow integral scale L becomes larger (and close to L_x) when $\gamma < \gamma^c$. This indicates that the inverse transfer of energy leads to the concentration of kinetic energy at large scales, and implies the formation of large structures in the flow (e.g., resulting from spatial aggregation of vortices). In the simulations varying A_z, we also verified that the overall shape of the quantities in the curves in Fig. 4 remain the same when changing the spatial resolution of the simulations, although the actual values (e.g., the time $t_{\rm max}$ or the maximum vortex length $l_{\rm max}$) depend on the resolution: at larger resolution the flow becomes more turbulent and vortex stretching is more efficient.

The numerical results show the existence of a transition between 2D and 3D behavior in quantum turbulence. This transition can be obtained by varying the dimensionality of the flow (in a 3D cubic domain), or by changing the aspect ratio of the domain and compactifying one spatial dimension. Below critical values of the controlling parameters the flows display an inverse transfer of energy which results in the growth of the incompressible kinetic energy at large scales, and in the aggregation of quantized vortices. For the quasi-2D regimes the system suffers an interesting double condensation: the BEC, and the out-of-equilibrium inverse energy cascade which can result in a condensation of the kinetic energy at the largest available scales in the system [12]. This behavior is compatible with critical transitions reported in classical turbulence [13–16], and reminiscent of recent observations in experiments of gaseous BECs [7–9]. For the 3D cubic domain, the critical amplitude of the 3D perturbation is $A_z^c \approx 10^{-2}$ (for the 512^3 simulations), while in the thin domains the critical aspect ratio is $\gamma^c \approx 1/10$. As our system is not forced, the inverse energy cascade can only develop as a transient (see, e.g., Ref. [23] for a discussion of the equivalent configuration in the classical case), a configuration which is comparable to experiments of gaseous BECs where the flow is let to freely decay after initially stirring it [1–3]. However, in experiments of gaseous BECs the condensate is trapped inside a potential, which

we are not considering in our simulations to increase the scale separation between the domain size and the vortex radius as much as possible. The study of the effect of trapping potentials in these cascades is left for future work.

N. P. M. and P. D. M. acknowledge financial support from grants UBACYT No. 20020170100508BA and Proyecto de Investigación Científica y Tecnológica (PICT) No. 2015-3530.

[1] E. A. L. Henn, J. A. Seman, G. Roati, K. M. F. Magalhães, and V. S. Bagnato, Phys. Rev. Lett. **103**, 045301 (2009).
[2] A. C. White, B. P. Anderson, and V. S. Bagnato, Proc. Natl. Acad. Sci. U.S.A. **111**, 4719 (2014).
[3] N. Navon, A. L. Gaunt, R. P. Smith, and Z. Hadzibabic, Nature (London) **539**, 72 (2016).
[4] W. F. Vinen and J. J. Niemela, J. Low Temp. Phys. **128**, 167 (2002).
[5] L. Skrbek and K. R. Sreenivasan, Phys. Fluids **24**, 011301 (2012).
[6] E. Fonda, D. P. Meichle, N. T. Ouellette, S. Hormoz, and D. P. Lathrop, Proc. Natl. Acad. Sci. U.S.A. **111**, 4707 (2014).
[7] S. W. Seo, B. Ko, J. H. Kim, and Y. Shin, Sci. Rep. **7**, 4587 (2017).
[8] G. Gauthier, M. T. Reeves, X. Yu, A. S. Bradley, M. A. Baker, T. A. Bell, H. Rubinsztein-Dunlop, M. J. Davis, and T. W. Neely, Science **364**, 1264 (2019).
[9] S. P. Johnstone, A. J. Groszek, P. T. Starkey, C. J. Billington, T. P. Simula, and K. Helmerson, Science **364**, 1267 (2019).
[10] T. Simula, M. J. Davis, and K. Helmerson, Phys. Rev. Lett. **113**, 165302 (2014).
[11] T. P. Billam, M. T. Reeves, B. P. Anderson, and A. S. Bradley, Phys. Rev. Lett. **112**, 145301 (2014).
[12] R. Kraichnan and D. Montgomery, Rep. Prog. Phys. **43**, 547 (1980).
[13] A. Celani, S. Musacchio, and D. Vincenzi, Phys. Rev. Lett. **104**, 184506 (2010).
[14] S. J. Benavides and A. Alexakis, J. Fluid Mech. **822**, 364 (2017).
[15] A. Alexakis and L. Biferale, Phys. Rep. **767–769**, 1 (2018).
[16] A. van Kan and A. Alexakis, J. Fluid Mech. **864**, 490 (2019).
[17] R. Gregory and R. Laflamme, Phys. Rev. Lett. **70**, 2837 (1993).
[18] See Supplemental Material at http://link.aps.org/supplemental/10.1103/PhysRevLett.124.134501 for a description of the Gross-Pitaevskii equations, of the initial conditions, of the fluxes and the determination of the total vortex length, and for videos of the time evolution of the system.
[19] P. D. Mininni, D. Rosenberg, R. Reddy, and A. Pouquet, Parallel Comput. **37**, 316 (2011).
[20] P. C. di Leoni, P. D. Mininni, and M. E. Brachet, Phys. Rev. A **95**, 053636 (2017).
[21] C. Nore, M. Abid, and M. Brachet, Phys. Fluids **9**, 2644 (1997).
[22] V. Shukla, P. D. Mininni, G. Krstulovic, P. C. di Leoni, and M. E. Brachet, Phys. Rev. A **99**, 043605 (2019).
[23] P. D. Mininni and A. Pouquet, Phys. Rev. E **87**, 033002 (2013).
[24] C. Nore, M. Abid, and M. E. Brachet, Phys. Rev. Lett. **78**, 3896 (1997).